Assessment of the reflectivity and emissivity impact on light metal roofs thermal behaviour, in warm and humid climate.

Jefferson Torres-Quezada ([1]*), Helena Coch ([1]), Antonio Isalgué ([2])

[1] Architecture, Energy and Environment, School of Architecture, Polytechnic University of Catalonia, Barcelona, Spain, Av. Diagonal, 649, 7th floor. 08028 Barcelona, Spain

[2]Applied Physics Department, Polytechnic University of Catalonia, Barcelona, Spain, Pla del Palau, 18. 08003

*Corresponding author: Jefferson Torres-Quezada; email: jefferson.torres@upc.edu

Abstract

The light metal roof is one of the roof typologies most used in low latitude regions with warm and humid climates. The low installation cost is one of the benefits of this typology, however, they offer only low resistance to the heat flux. In order to analyse strategies to reduce the indoor overheating in this climates, this investigation addresses the impact of reflectivity and emissivity on the light metal roof thermal behaviour. The study was carried out with dynamic simulations, considering the climate of a city in the south coast of Ecuador (Santa Rosa, 3°27´S). This analysis has parameterized the interior surface temperature in function of the reflectivity and emissivity, which has been validated with the measurements of several samples with different radiative properties. The analysed samples show that the effect of the aging and the use of different paints have a higher impact on the increase in emissivity than on reflectivity. In conclusion, the results show that the radiative parameter with the highest influence on interior surface temperature reduction is emissivity.

Keywords: metal roof, solar reflectivity, thermal emissivity, warm and humid climates.

1. Introduction.

The regions located near to the equator are characterized by high temperatures, humidity and especially high global solar radiation [1] [2]. Due to the angle of sun rays in this zone, the roof is the part of the envelope most exposed to solar flux throughout the year. Despite solar paths being nearly the same for different regions within these latitudes, cities that are located near the sea have a high relative humidity, while cities farther away from the sea have less cloudy conditions [3] [4].

The importance of roofs on interior conditions depends on the urban context and the building morphology [5] [6]. The constant and hasty growth of the world urban population in the last decades has brought as a consequence a sharp increase of residential demand [7], and with it, the increase of energy consumption, especially in low latitudes countries [8] [9]. In the cities of these regions, which have adopted an urban sprawl model [10], the most extended building typology is the low rising building.

Hence, the roof surface represents 32% of the whole building envelope. As a result, the roof, within this climatic and urban context, is the main source of heat gains (54%) in buildings of these regions, even higher than window solar gains [11].

One of most the important parameters for the user interior thermal conditions is the mean radiant temperature (*Tmrt*) [12] [13]. This parameter has a similar importance as the indoor air temperature (*Ta*) on the user thermal perception [14]. Due to the high proportion of the roof with respect to the interior space, the interior surface temperature of this element can determine *Tmrt* [15] [16].

Nomenclature

Tmrt	Mean radiant temperature
Ta	Outdoor air temperature
Ts	Exterior surface temperature
Tsi	Interior surface temperature
MR	Light metal roof
MR_new	Metal roof in new state
MR_old1	Metal roof with 1 year installed
MR_old2a	Metal roof with more than 5 years installed (sample a)
MR_old2b	Metal roof with more than 5 years installed (sample b)
MR_old2c	Metal roof with more than 5 years installed (sample c)
MR_cool	Metal roof painted with cool roof paint
MR_white	Metal roof painted with white paint
MR_green	Metal roof painted with green paint

In regions at these latitudes, the most commonly used roof is the light metal roof (MR), as in Malaysia [17], Indonesia [18], and especially in countries from Central and South America: Costa Rica [19], Dominican Republic [20], or Ecuador. In the warm humid Region of this last country, 65% of the entire residential buildings use this typology of roof [21]. A major benefit of this typology is the low installation cost. However, due to its low thickness and its thermal properties, this roof has a low resistance to the heat flux.

In order to reduce the overheating conditions in buildings of these regions, an analysis of the strategies applied to the light metal roof (MR) is necessary. Among the parameters that modify the thermal behaviour of the roof are the solar reflectivity and thermal emissivity of the surface material, where especially the reflectivity factor has high repercussions on indoor overheating reduction [22] [23] [24] [25]. The solar reflectivity refers to shortwave reflected by the roof (wavelengths inferior to 4 µm, nearly 50% of which in the visible spectrum and 50% in the near infrared), and, the thermal emissivity refers to the long wave radiation emitted by the roof (wavelengths superior to 4 µm or far infrared) [5]. So, the interior surface temperature (*Tsi)* largely depends on the balance of these two fluxes. Nevertheless, the aging and the exposition to the outdoor environment modify these a [26], which significantly influences the thermal performance of the roof.

Therefore, this work deals with the thermal behaviour of the light metal roof (MR) in warm humid climate of low latitude regions. The specific objective of this research is to evaluate the repercussions of modifying solar reflectivity and thermal emissivity on this roof interior surface temperature (*Tsi*).

2. Methodology

The method of this investigation was carried out in a three-step process. The first part consists of *in situ* measurements of climatic factors and thermal parameters of a light metal roof (MR). The second part focuses on the simulation of the roof thermal behaviour, using as input data all the parameters measured before in the first part. In the last part, measurements of several samples of this roof typology have been used to validate the results obtained in the simulations. Once the simulations have been validated, conclusions can be drawn from these results.

2.1 Measurements of Input Data

The measurement campaign was conducted in Santa Rosa, a city in the south coast of Ecuador, at latitude 3°27´S and altitude 14masl. A total of 70% of residential buildings in this city are only one floor high [21], and the most used roof material is the metal sheet as shown in Fig. 1.

Fig. 1 Aerial view (left) and street view (right) of Santa Rosa city in Ecuador. Images retrieved from google maps.

This region is characterized by its warm-humid climate throughout the whole year. The mean temperature is 26°C, with a daily and annual oscillation of 6°C and 4°C respectively; and the mean relative humidity in the year is 85% as illustrated in Fig. 2.

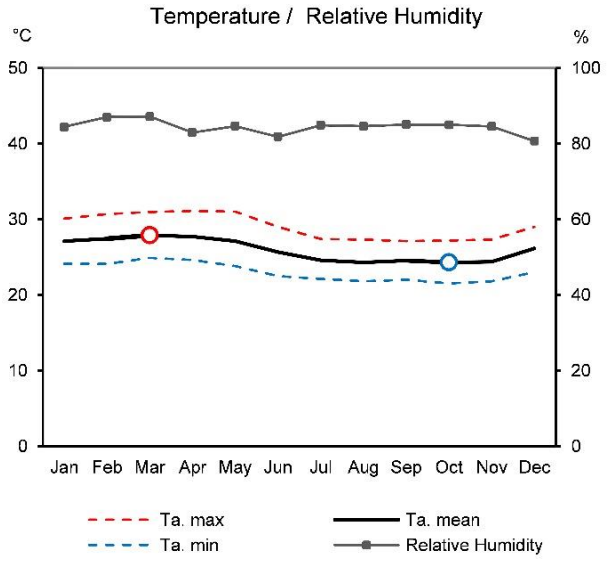

Fig. 2 Monthly average of: mean, maximum and minimum air temperature, and relative humidity of Santa Rosa city-Ecuador. Data collected from meteorological station [27].

The climatic factors measured are: air temperature, humidity, air velocity, solar radiation, cloud cover and sky temperature. Data measurements for all these factors, except sky conditions, were gathered from a meteorological station (ID: IELOROEL2) located at 15 km from Santa Rosa (3°18´3´´S, 79°53´53´´O, 20 masl) [30]. The technical specification of the meteorological station corresponds to a Davis Vantage Pro2 Plus (Wireless). These data were collected during the entire year 2016 in 15 min intervals. With respect to sky conditions, the cloud cover factor, which is defined as the fraction of the sky vault covered by clouds [28], was measured with the method of observation [29] [30]. In addition, solar radiation with clear sky conditions has been simulated with the use of the software Heliodon [31]. The sky temperature measurements were carried out using an infrared thermometer TESTO 830 T4 with a range of -30°C to +400°C. Due to the fact that the sky is not uniform, the sky temperature was measured in different points of the sky vault, from the skyline to the zenith. These measurements were used to obtain an average of the sky temperature. The cloud cover and the sky temperature were captured at 2 hours intervals during 7 days in October and December of 2016.

Based on statistical analysis of all the data collected in this year, climatic factors have been obtained of a day that represents the mean extreme heat conditions in this region. Nevertheless, the whole data

obtained from these measurements are detailed in supplementary Table 1 and supplementary Table 2 in Ref [52].

The measured MR belongs to a residential building located in Santa Rosa city. The specific characteristics of this roof correspond to a 0.3mm galvanized steel sheet and covered by an alloy of aluminium and zinc (55%-45%) [32] [33]. According to the manufacturer and bibliography, this material, in its original new state, has a solar reflectivity of around 0.75 and thermal emissivity of around 0.12 [34] [35] [36]. However this roof had been installed more than 5 years before the measurements, thus, its current state is dusty and old but not rusted. Because of these circumstances, it is necessary to measure the reflectivity and the emissivity of this roof in the current conditions, Fig. 3.

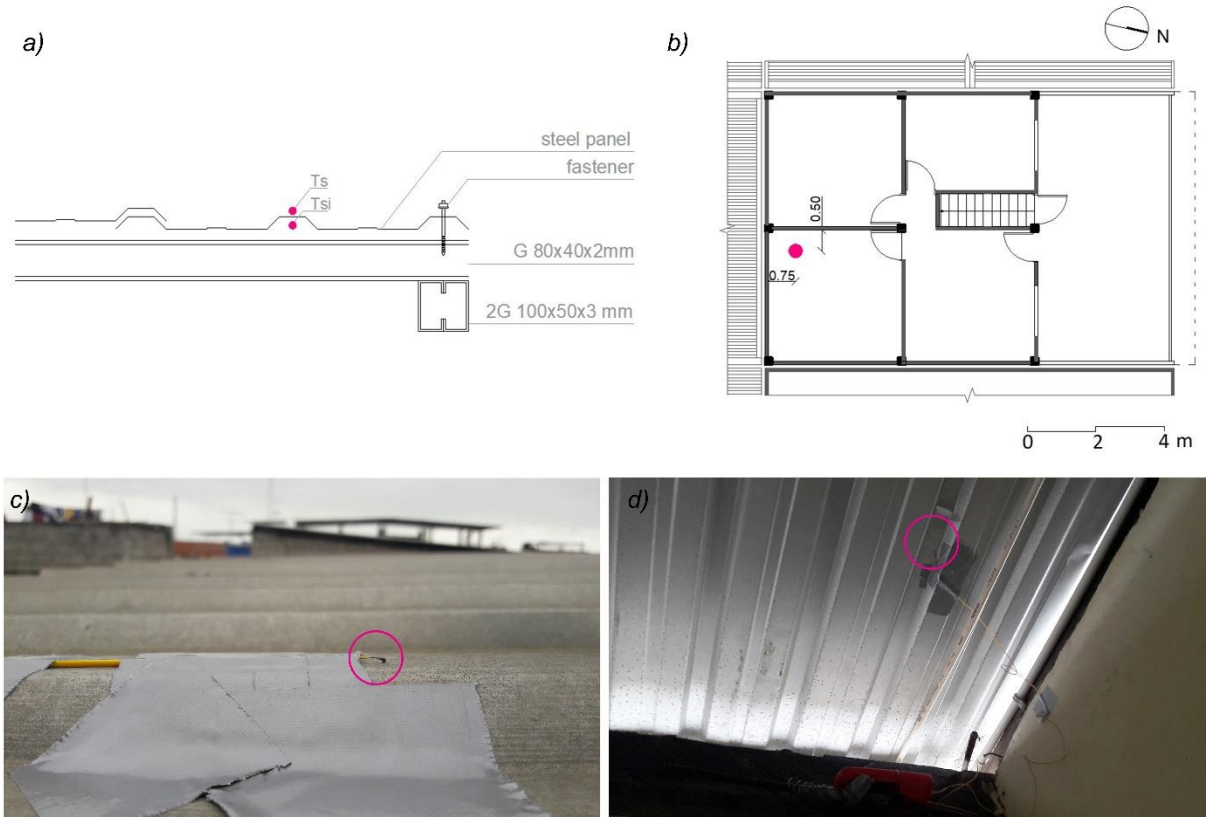

Fig. 3 Light metal roof constructive detail (a), floor plan with the thermocouple position (b), outside (c) and inside (d) surface temperature measurements.

The measured roof parameters are the visible reflectivity, thermal infrared emissivity, as well as the exterior (*Ts*) and interior surface temperature (*Tsi*). The measurement methods of the reflectivity and emissivity of this roof are based on previous works from [37] [38] [39] [40] and [41]. Due to the high conductivity of the metal roof and its low thickness, the exterior and interior surface temperature are the same. The same results were obtained in other studies [42] [43]

The process to measure the reflectivity consisted in comparing the MR surface with a reference surface by capturing photographic images, which were taken at angles of less than 45º from the normal to the

surface to minimize the error of the measurements [38]. Each image was processed through a graphics software (Adobe-Photoshop) [44] to obtain the optical histogram of the sample and the reference surface. The reference surface used for this comparison was a sheet of 100% opaque white paper. Assuming that the surface has a fully Lambertian reflection, the reflectance factor of this surface was obtained through Eq. 1.

$$r = \frac{\pi . L}{E} \qquad Eq.1$$

Where r is the reflection factor, L is the luminance value (cd / m^2) and E the illuminance value (lux). The values of L and E were obtained through measurements. The instruments used to measure the parameters were a Light meter LX1010B lux meter, and a Konica Minolta LS 110 Luminance meter. The solar reflectance obtained from the reference surface (white paper) was 0.85.

In order to measure emissivity, the process consisted of simultaneously measuring the exterior surface temperature and exterior radiant temperature of the roof, using a multi-logger thermometer Amprobe TMD 56 with a thermocouple type K, and an infrared camera (adjusted to an emissivity of 1.00), respectively. Two infrared cameras were used for this process: a FLIR I7 and an InfRec H2640. In one hand, the measurements were made *in situ* in Santa Rosa-Ecuador with the use of FLIR i7 infrared camera. In order to validate the field results, additional measurements were carried out in the laboratory, where the infRec H2640 has been used.

The taking of measurements with both cameras were made with angles lower than 45° with respect to the normal to the surface. Then, using the software of these cameras (FLIR Tools, Infrarec Analyzer Lite), the radiant temperature (infrared camera) was equalized to the surface temperature (thermometer) according to the change in the emissivity value. By achieving the equality of their temperatures, the emissivity of this surface was obtained.

The emissivity measurement procedure was based on the standard Test Methods for Measuring and Compensating for Emissivity Using Infrared Imaging Radiometers: contact thermometer method [41]. The apparent temperature was configured with an emissivity value of 1.00. The reflected temperature was assumed as the sky temperature for measurements made *in situ,* as well as the air temperature was set for laboratory measurements. Both measurements give quite similar emissivity values, with a variation between them of less than 3%. The values used for the analysis of each sample were the average of two measurements.

The interior and exterior surface temperatures were measured with the same multi-logger used to measure the emissivity. The data was gathered in 10 min intervals during 10 days in October and 10

days in December of 2016. The purpose of these field measurements was the validation of the simulated results.

2.2 Simulations

The second part of the methodology is based on dynamic simulations with the use of the Design Builder interface [45], which uses Energy Plus as a calculation engine [46]. The EPW file (Energy Plus Weather) used for these simulations were set by using the data collected in the measurements campaign carried out in October and December (see supplementary Table 3 in ref [52]. From these simulations, one day (October 10th) with the characteristics coincident with the day with mean extreme heat conditions from the whole year was chosen to analyse. The purpose of choosing this day is to show the extreme effect of the radiative properties of the light metal roof.

Furthermore, a simulation model has been established, where the roof thermal parameters were set according to the values obtained in the measurements. Additionally, the geometry, materials, orientation and urban typology of this model were configured based on the predominant characteristics in these regions, where the low height floor is the predominant building typology, the use of light block is the most used material for walls and the typical plot of land is 9m x 9m [47]. Following these characteristics, the model is a one-floor residence of 9m x 9m x 3.1m height, attached to equal buildings by its North and South sides. The model has been divided into 9 subzones (spaces), through a 3 x 3m grid. The subdivision of this model resembles the buildings structural characteristics in these regions, where the typical inter-columns distance is 3m. In order to avoid the influence of direct solar radiation, the model does not include glass surfaces and only the central space has been evaluated, see Fig. 4. In regards to the infiltrations and the occupation values were set according to the collected data in situ. Infiltrations were approached by measuring CO2 concentrations in a windowless room. The measurements were taken by several hours, following the Tracer Gas process specified in [48]. The values obtained from these measurements were confronted with the simulation software and were in agreement. All the simulation parameters are shown in Table 1.

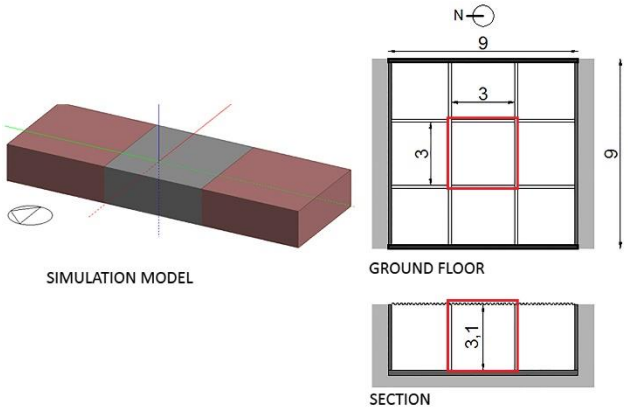

Fig. 4 Simulation Model

Roof	
Reflectivity	0.10 – 1.00
Emissivity	0.10 – 1.00
Thermal mass	0.65 kJ/m^2.K
Thermal transmittance	7.40 W/m^2.K
Walls-thermal transmittance	3.20 W/m^2.K
Floor-thermal transmittance	1.96 W/m^2.K
Occupancy	Constant 0.04 people/m^2
Infiltrations	Constant 0.7 ac/h
Ground Temperature	25.80°C

Table 1 Simulation parameters

Finally, with the use of the simulation model, the interior surface temperature of this roof has been parameterized as a function of changes in the reflectivity and emissivity parameters.

2.3 Validation

The next part of this methodology is the validation of the simulation results. First of all, the radiative properties from several samples of the light metal roof (MR) have been measured. After this, the surface temperatures of these samples have been simulated. Finally, the surface temperatures of these samples have been measured and compared with the simulated results.

The samples measured correspond, on the one hand, to roofs of this typology in their unpainted state with different weathering, and on the other hand, to roofs with different paints coatings.

About the unpainted set, it has measured 3 different states of weathering: a sample in a new state (MR_new), a sample with 1 year installed (MR_old1), and 3 samples with more than 5 years installed (MR_old2a, MR_old2b and MR_old2c). Despite that the 3 oldest roofs have approximately the same age, they belong to three different houses which were exposed to three different conditions of weathering. These roofs were measured to have a larger number of samples to analyse the tendency of radiative parameters influenced by the aging. MR_olda corresponds to the metal roof of the measured residential building.

While the painted set consists of: a sample with cool roof paint coating (MR_cool), a sample with white paint coating (MR_white) and a sample with green paint coating (MR_green).

The reflectivity, the emissivity and the surface temperature of all these samples have been measured with the same methods and the same instrumentation as mentioned before. The specific characteristics of all measured samples are shown in Table 2.

Roof sample	Graphic code	Specifications	Real State
MR_new	○	Unpainted state	Clean
MR_old1	○	Unpainted state	Dusty
MR_old2a	○	Unpainted state	Dusty
MR_old2b	○	Unpainted state	Dusty
MR_old2c	○	Unpainted state	Dusty
MR_cool	□	Cool Roof paint	Clean
MR_white	□	White paint	Clean
MR_green	□	Green paint	Clean

Table 2 List of the all measured samples.

The comparison between simulated data and the on-site measurements is shown in Fig. 5, which reveals that the maximum difference between them is 1.5ºC out to (Tmax – Tmin) = 36ºC.

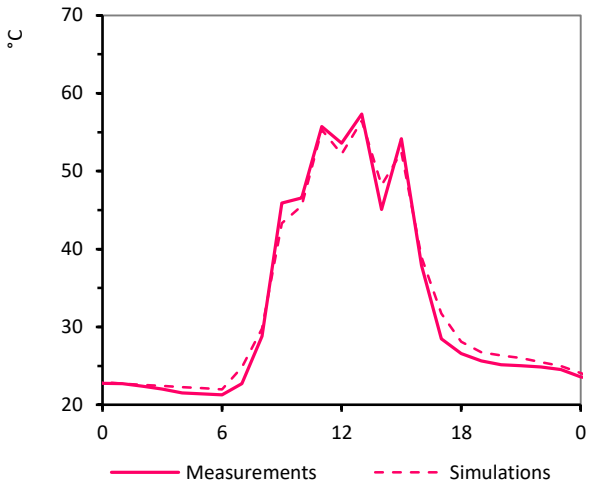

Fig. 5 Interior surface temperature of the residential building metal roof obtained by measurements and simulations, during a day with extreme heat conditions in these regions.

Finally, once the simulated results have been validated, the computation can be used to draw conclusions for this climate.

3. Results and discussion

3.1 Measurements

From the measured data, the climatic factors for a day with extreme heat conditions are shown in Fig. 6. According to all the data collected, this day represents 20% of the total number of days analysed in this year. In addition, this figure shows the simulated solar radiation with clear sky condition, with the purpose to evidence the high influence of the cloudiness on solar radiation.

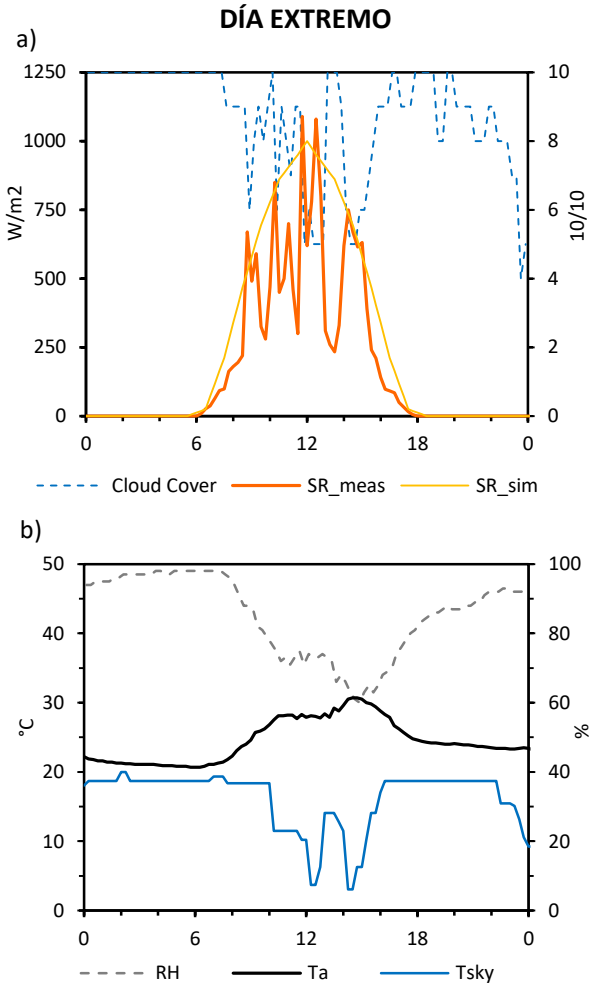

Fig. 6 Climatic factors of a day which describe extreme heat conditions in this region, a) measured cloud cover, measured global solar radiation and simulated solar radiation with clear sky conditions. b) Relative humidity, outdoor air temperature and sky temperature.

The results show a very inconstant and irregular measured solar radiation (SR_meas), which reflects the cloudy sky conditions throughout the whole day. The peak solar radiation in this day is 1075 W/m^2, when the cloud cover is 5/10. However, when this sky condition increases to 10/10, at 13h30, the solar radiation reduces to 230 W/m^2. Furthermore, according to these results, most of these measured values are lower than simulated solar radiation values (SR_sim). This behaviour reveals the great influence of cloud cover on the amount of solar radiation received.

Moreover, high levels of cloud cover are also shown during night-time. In the first night period (00h00 – 06h00), the sky is totally covered with 10/10. Although in the second night period (18h00 – 24h00) the levels of sky cover are lower than in the first period, the average is still very high with 8/10. This climatic condition directly affects the radiative cooling capacity of the sky, especially in this period. According to Fig. 6b, the sky temperature, in both night periods, is around 18°C, among 3°C and 6°C below air temperature. Meanwhile, in the day-time, the lowest sky temperature is 3°C, which coincides with the lowest cloud cover in this period (5/10). According to these data, the difference between air temperature and sky temperature is low, especially in the night period. Thus, the flux by long wave radiation emitted to the sky is limited in this region.

Regarding the measurements of the roof parameters, the interior surface temperature of the residential building roof (MR_olda) is shown in Fig. 7. These results correspond to the chosen day with extreme heat conditions. In order to put some reference parameter for the behaviour of the roof temperature, this figure also shows the outdoor air temperature measured in this day (*Ta*). According to the radiative properties measurements of this roof, its reflectivity is 0.52 and its emissivity is 0.30.

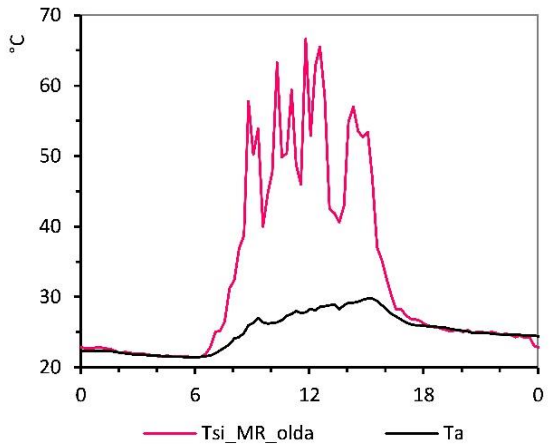

Fig. 7 Measured interior surface temperature of the residential building metal roof (Tsi_MR_olda) and measured outdoor air temperature (Ta) during a day with extreme heat conditions in these regions.

The interior surface temperature of the MR_olda shows a behaviour very similar to the solar radiation Fig. 6a, which reflects the high influence of this flux on the roof temperature. In the solar radiation peak, MR_olda reaches an interior surface temperature of 66°C, and when solar flux reduces to 230 W/m^2 (at 13h30), this temperature straightaway reduces to 40°C. Moreover, when the solar radiation disappears, the temperature of MR_olda is immediately reduced to the same temperature of the air (*Ta*), around 26°C. MR_olda maintains the same temperature as air throughout the whole night-time. Due to the low emissivity of this roof, in addition to the low cooling capacity of the sky, heat losses by long wave radiation are minimal, and consequently, the interior surface temperature of the MR_olda is not reduced

below *Ta* almost at any time, as it happens in other climates and other roofs with higher emissivity [49] [50] [51].

Furthermore, the reflectivity and emissivity values of all measured samples are shown in Table 3, and Fig. 8.

Roof sample	Graphic code	Reflectivity	Emissivity
MR_new	○	0.75	0.13
MR_old1	◎	0.63	0.26
MR_old2a	◎	0.52	0.30
MR_old2b	◎	0.52	0.50
MR_old2c	◎	0.57	0.65
MR_cool	□	0.86	0.90
MR_white	□	0.77	0.95
MR_green	□	0.25	0.95

Table 3 Reflectivity and emissivity measured values of all samples

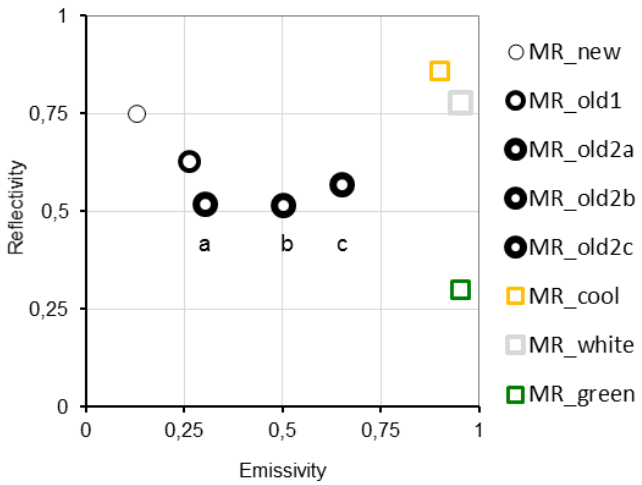

Fig. 8 Reflectivity and emissivity measured values of metal roof samples in its original state with different aging (circles), and metal roof samples with different paint coatings (squares).

All the samples in their unpainted state with different weathering show a reduction in their reflectivity, with respect to the metal roof in its new state (MR_new). However, they also show an increase in their emissivity. The polished and smooth of the metal roof becomes a surface with higher roughness, due to the accumulation of dust and other chemical processes, thus, its emissivity is increased.

Samples with more than 5 years of installation (MR_old2a, MR_old2b, MR_old2c) present a reflectivity reduction of 0.23, 0.23 and 0.18 respectively. However, the same samples show an emissivity increase of 0.17, 0.37 and 0.52 respectively. In the case of MR_old1, the sample with only 1 year of installation, have a similar behaviour: a reflectivity reduction of 0.12 and an increase in its thermal emissivity of 0.13. According to these results, the general effect of aging on the light metal roof has a higher impact on the increase of its emissivity than on the reduction of its reflectivity. The highest reflectivity reduction is 0.23, from 0.75 to 0.52, while, the highest emissivity increase is 0.52, from 0.13 to 0.65. Based on the data analysed, the average relation between the reflectivity decrement and the emissivity increment is 1:1.6. In regard to the samples with paint coating, the results show that painting the metal roof changes significantly its radiative properties with respect to all samples in their original state. In comparison to the metal roof in its new state (MR_new), the reflectivity can change in both ways, while the emissivity only increases.

MR_cool and MR_white show an increase in both factors, in their reflectivity 0.11 and 0.03, and in their emissivity 0.77 and 0.82 respectively. MR_green shows a reflectivity reduction of 0.50, and an emissivity increase of 0.82. According to these results, the paint coating on the metal roof has a low impact on the increase of its reflectivity, however, it shows a high repercussion on the increase of its thermal emissivity.

The thermal response of the radiative parameters of these two samples set is discussed in a later section.

3.2 Simulations

Once the EPW file was set according to climatic data of the chosen day, and the roof parameters were configured agreeing to the measurements, the interior surface temperature of the metal roof (*Tsi*_MR) has been parameterized in function of the reflectivity and the emissivity as presented in Fig. 9. This figure uses a colour scale to represent the behaviour of the *Tsi*_MR. Every colour band indicate a common area of temperature “isotherms”. Every isotherm represents an interval of 2°C. The Y-axis shows the values of the reflectivity, and the X-axis shows the values of the emissivity. The range of both parameters goes from 0.10 to 1.00. According to this representation, the lowest temperatures are represented with cyan colours in a range of 20-22°C, and the highest temperatures are represented by the purple colour in a range of 54-56°C. The results have been divided into two periods: day-time and night-time, thus, the *Tsi*_MR has been analysed with the average in every period. Due to the geographic location of this city (near latitude 0°) both periods have the same number of hours throughout the year,

12h. Daytime lasts from 06h00 to 18h00 and night time comprises two semi-periods from 00h00 to 06h00 and 18h00 to 24h00. The same colour scale is used for both periods.

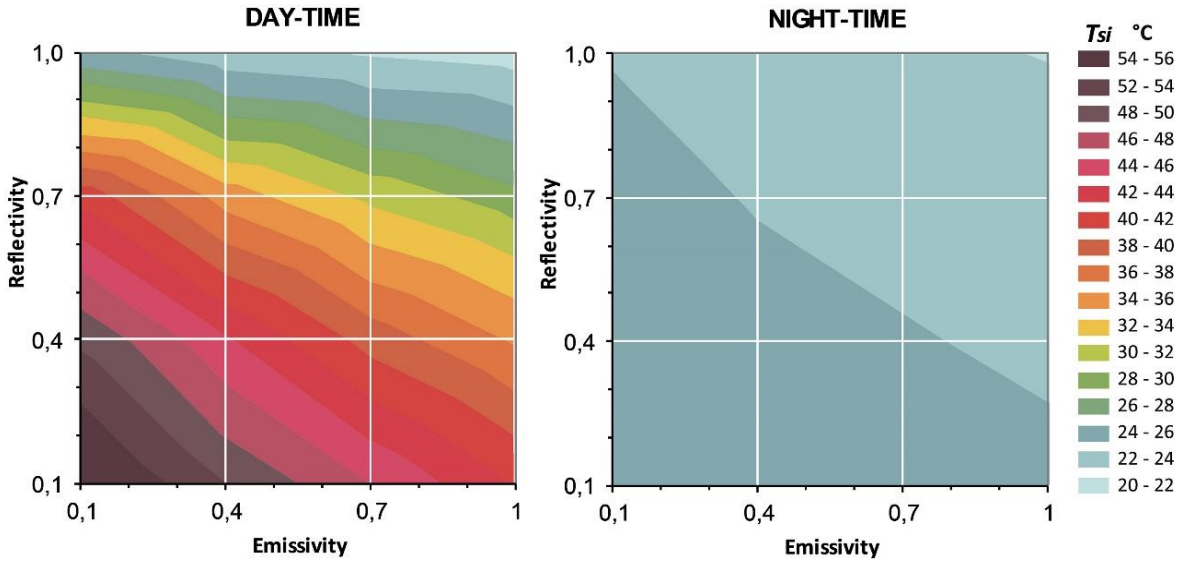

Fig. 9 Parameterization of Tsi_MR in function of the reflectivity and emissivity, in day and night-time period.

During day-time, both radiative parameters show a large influence on *Tsi*_MR. The maximum variation is 36°C, between the lowest (r=0.10 e=0.10) and the highest (r=1.00 e=1.00) values of both parameters. Nevertheless, the reflectivity has a greater impact on this variation than emissivity. On the one hand, the increment of the reflectivity from 0.10 to 1.00, with the lowest emissivity 0.10, represents a temperature reduction of 32°C. The reflectivity impact on *Tsi*_MR is less important according to emissivity increase. The increase of the reflectivity from 0.10 to 1.00, with the highest emissivity 1.00, shows a temperature reduction of 22°C. On the other hand, the increment of the emissivity from 0.10 to 1.00 only represents a temperature reduction of 12°C and 6°C, with the lowest and highest reflectivity value (0.10 and 1.00) respectively.

On the contrary, in the night period, the influence of the reflectivity and emissivity on *Tsi*_MR is minimal. This time, the maximum variation is only 4°C, between the lowest (r=0.1 e=0.1) and the highest (r=1.00 e=1.00) values of both parameters. In spite of the absence of solar flux in this period, the reflectivity factor shows some impact on *Tsi*_MR. This is because of the heat stored within the indoor space. Additionally, in this period, the emissivity is the only parameter that has a direct influence on the roof balance, however, due to the low cooling capacity of the sky, the impact of this factor on the reduction of *Tsi*_MR is minimal, even with high values.

3.3 Measured thermal response of roof radiative parameters

The thermal response (*Tsi*) of the radiative parameters of all the samples analysed before (see Fig. 8) has been visualized with the isotherms graph, as seen in Fig. 10. These results were validated with the temperature of every sample obtained by measurements. All samples are going to be analysed in comparison to the sample in its new state.

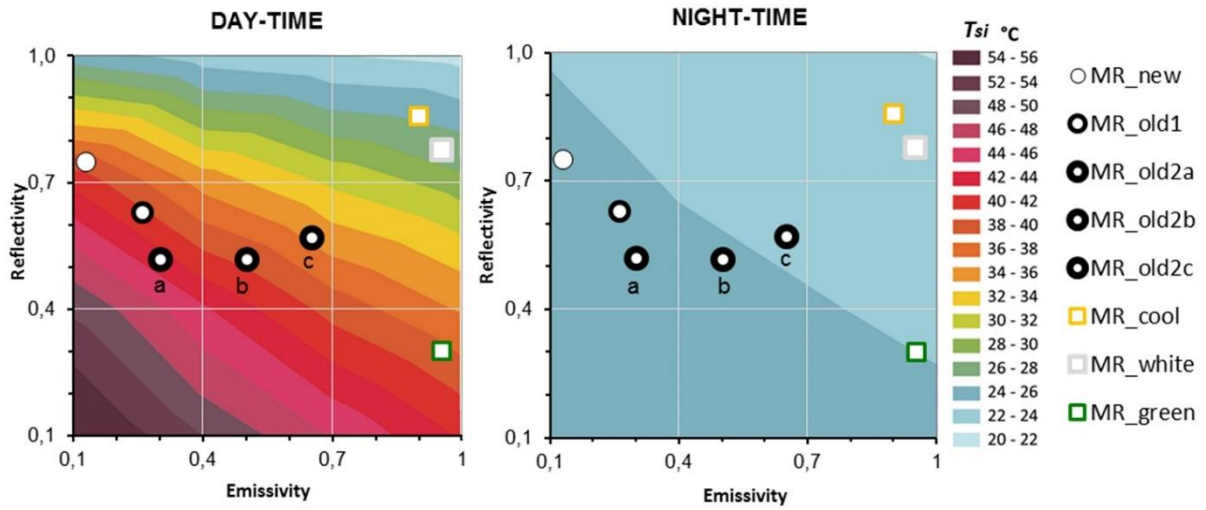

Fig. 10 The thermal response (Tsi) of the radiative parameters of all analysed samples: metal roof samples in its original state with different weathering (circles), and metal roof samples with a coating of paint (squares).

With respect to the samples in their unpainted state with different weathering, during day-time, the *Tsi* of the sample in its new state (MR_new) is 39°C, while for the sample with one year of installation (MR_old1) the *Tsi* is 40°C, and for the samples with more years of use (MR_old2a, MR_old2b, MR_old2c) the *Tsi* is 43°C, 39°C and 35°C respectively. While for night-time, all samples have a temperature slightly higher than 24°C, with the exception of MR_old2c which is below 24°C.

According to these results, the metal roof with the lowest temperature in both periods is the sample with the highest value of emissivity, (MR_old2c), which is one the samples with more years of installation. The temperature of this sample is even lower than the metal roof sample in its new state (MR_new), which has a higher reflectivity but a lower emissivity. Even MR_old2b, one of the sample with the lowest reflectivity but with an emissivity of 0.52 has the same temperature as MR_new. In the case of MR_old1 and MR_old2a, due to they have the lowest emissivity increase, their temperatures show an increase compared to MR_new. Nevertheless, these temperatures are only 1°C and 3°C higher than MR_new respectively.

In consequence, since the effect of the aging has a greater impact on the emissivity increase than on the reflectivity reduction, the metal roofs with several years of use tend to have similar temperatures

than these roofs in their new state, and eventually, in function on the increase of their emissivity, they show a lower temperature.

Regarding the samples with different paint coatings, during day-time, the white painted sample (MR_white) has an interior surface temperature of 27°C, while the cool roof painted sample has a temperature of 26 °C, and the green painted sample of 36.5°C.

According to these results, the roofs with the lowest temperatures of all the analysed samples in both periods are MR_cool and MR_white. Due to their increased of reflectivity and especially emissivity, in comparison to the metal roof in its new state, these samples have a temperature of 16°C and 14°C lower than MR_new respectively. Even, with a lower reflectivity, MR_green has the same temperature as MR_new during day-time and a lower temperature during night-time, due to the high increase of its emissivity.

In consequence, since the use of paint coating on light metal roofs has a large impact on the emissivity increment, these samples tend to have a lower temperature in comparison to the roofs in their new state, even when using paints with lower values of reflectivity.

Based on the analysed samples, the greatest impact on the reflectivity reduction due to the aging is by 0.23, from 0.75 down to 0.52, which represents a temperature increment of 4°C, while, the greatest impact on the emissivity increasing is by 0.52, from 0.13 up to 0.65, which results in a temperature reduction of 12°C. Furthermore, the changes caused by the use of paint show a maximum reflectivity increase of 0.11, from 0.75 up to 0.86, which represents a temperature reduction of 8°C. While, the maximum emissivity increase is 0.82, from 0.13 up to 0.95, which results in a temperature reduction of 14°C.

Although the general parametric analysis shows that the reflectivity has greater repercussions on the roof thermal behaviour than emissivity, the results of both samples set show that the emissivity stands out as the radiative parameter with the highest impact on the *Tsi* reduction of the MR.

4. Conclusions

The central scope of this research has been the thermal behaviour of light metal roofs in latitudes near to Equator with warm and humid climates. This roof typology has been widely disseminated in these regions despite of the general opinion is that it provides a high indoor overheating. This investigation has been developed from the radiative perspective, considering both the short wave radiation and the long wave radiation. In order to accomplish the aim of this investigation, a set of results have been obtained through simulations based on measurements carried out in a city on the coast of Ecuador.

The simulations have been validated with further measurements of several samples of this roof typology. From these results some conclusions can be mentioned:

The reflectivity and emissivity have large repercussions on the light metal roof interior surface temperature during day-time, while, during night-time, the influence of these radiative parameters is minimal. Due to the low cooling capacity of the sky in this region, even the maximum increase in emissivity has a minimal impact on the interior surface temperature reduction during the night period.

Finally, contrary to what is generally believed, a light metal roof with low reflectivity and high emissivity tends to have a lower temperature than a roof in its new state. Even, an old roof with high emissivity may have a lower surface temperature than a new roof, apparently more reflective to sunlight. Therefore, since the capacity of the light metal roof to increase its emissivity with the use of simple methods such as common commercial paints or its own aging, make this type of roof a viable option in construction in climates similar to the studied in this research.

Acknowledgments

Work supported by Spanish Ministry of Economy, project code: BIA2016-77675-R. JTQ acknowledges scholarship AR6C9307 from the government of Ecuador. Part of this work is part of the PhD Thesis of Dr J.Torres.

References

[1] Atkinson, G. A. (1950). Building in the Tropics, Royal Institute of British Architects, 57, pp. 313–319.

[2] Edmonds, I. R. and Greenup, P. J. (2002). Daylighting in the tropics, Solar Energy, 73(2), pp. 111–121. https://doi.org/10.1016/S0038-092X(02)00039-7

[3] Serra, R. y Coch, H. (2001). ARQUITECTURA Y ENERGÍA NATURAL. Barcelona: Edicions UPC.

[4] Beckers, B. (2012). Solar energy at urban scale. Hoboken : John Wiley & sons.

[5] Diulio, M. de la P., Netto, G. R., Berardi, R. and Czajkowski, J. D. (2016). Impact of the envelope on residential heating energy demand in the Metropolitan Region of La Plata, based on the energy retrofit of a house, Ambiente Construido, 16(1). http://dx.doi.org/10.1590/s1678-86212016000100060

[6] Jim, C. Y. (2015). Diurnal and partitioned heat-flux patterns of coupled green-building roof systems, Renewable Energy, 81, pp. 262–274. http://dx.doi.org/10.1016/j.renene.2015.03.044

[7] United Nations, Department of Economic and Social Affairs, P. D. (2015). World Urbanization Prospects: The 2014 Revision,(ST/ESA/SER.A/366).

[8] Levine, M., D., Ü.-V., K., B., Geng L., H. D., S., L., G., L., A., M. M., S., M., A., N., J., R. and Yoshino H. (2007). Residential and commercial buildings. In Climate Change 2007: Mitigation. Contribution of Working Group III to the Fourth Assessment Report of the Intergovernmental Panel on Climate Change [B. Metz, O.R. Davidson, P.R. Bosch, R. Dave, L.A. Meyer (eds)]. Cambridge, United Kingdom and New York, NY, USA.

[9] Liu, F., Meyer, A. S. and Hogan, J. (2010). Mainstreaming building energy efficiency codes in developing countries : global experiences and lessons from early adopters. Washington, DC: World Bank. https://doi.org/10.1596/978-0-8213-8534-0

[10] Downs A (1999). Some Realities about Sprawl and urban decline, Housing Policy Debate, 10(4), pp. 955–974. https://doi.org/10.1080/10511482.1999.9521356.

[11] Torres-Quezada, J., Coch, H., Isalgué, A. and López, J. (in press). The roof impact on the heat balance of low height buildings at low latitudes. In PLEA: Smart and Healthy within the 2-degree limit.

[12] Kalmár, F., Kalmár, T. (2012). Interrelation between mean radiant temperature and room geometry, Energy and Buildings, 55, pp. 414–421. https://doi.org/10.1016/j.enbuild.2012.08.025

[13] d´Ambrosio, F., Dell´Isola, M., Palella, B., Riccio, G. and Russi, A. (2013). On the measurement of the mean radiant temperature and its influence on the indoor thermal environment assement, Building and Environment, 63, pp. 79-88. http://dx.doi.org/10.1016/j.buildenv.2013.01.026

[14] Walikewitz, N., Britta, J., Langner, M., Meier, F. and Endlicher, W. (2015). The difference between the mean radiant temperature and the air temperature within indoor environments : A case study during summer conditions, Building and Environment, 84, pp. 151–161. http://dx.doi.org/10.1016/j.buildenv.2014.11.004

[15] Atmaca, I., Kaynakli, O. and Yigit, A. (2007). Effects of radiant temperature on thermal comfort, Building and Environment, 42(9), pp. 3210–3220. http://dx.doi.org/10.1016/j.buildenv.2006.08.009

[16] Torres-Quezada, J., Coch, H., Isalgué, A. and Crespo, I. (2017). Experimental study of the roof thermal performance influence over the mean radiant interior temperature of an industrial building. In PLEA Conference Proceedings: Design to Thrive, 3, pp. 3810–3817.

[17] Allen, L. K. K., Elias, S. and Lim, C. H. (2008). Thermal Performance Evaluation of roofing systems and materials in Malaysian residential development. In Proceedings of SENVAR, ISESEE, Humanity and Technology, pp. 387–395

[18] Lauber, W., Cheret, P., Ferstl, K. and Ribbeck, E. (2005). Tropical architecture : sustainable and humane building in Africa, Latin America, and South-East Asia. New York: Prestel.

[19] INEC (2011). X Censo Nacional de Población y VI Vivienda de 2011. Available at: http://sistemas.inec.cr:8080/bincri/RpWebEngine.exe/Portal?BASE=2011&lang=esp (Accessed: March 3, 2018).

[20] OficinaNacionaldeEstadística(ONE). (2010). IX Censo Nacional de Población y Vivienda 2010. Available at: http://redatam.one.gob.do/cgibin/RpWebEngine.exe/PortalAction?&MODE=MAIN&BASE=CPV2010&MAIN=WebServerMain.inl (Accessed: March 3, 2018).

[21] INEC (2010). CENSO DE POBLACIÓN Y VIVIENDA 2010. Available at: http://redatam.inec.gob.ec/cgibin/RpWebEngine.exe/PortalAction?&MODE=MAIN&BASE=CPV2010&MAIN=WebServerMain.inl (Accessed: May 1, 2016).

[22] De Brito Filho, J. P., Henriquez, J. R. and Dutra, J. C. C. (2011). Effects of coefficients of solar reflectivity and infrared emissivity on the temperature and heat flux of horizontal flat roofs of artificially conditioned nonresidential buildings, Energy and Buildings, 43(2-3), pp. 440–445. https://doi.org/10.1016/j.enbuild.2010.10.007

[23] Synnefa, A., Saliari, M. and Santamouris, M. (2012). Experimental and numerical assesment of the impact of increased roof reflectance on a school building in Athens. Energy and Buildings, 55, pp. 7-15. https://doi.org/10.1016/j.enbuild.2012.01.044

[24] Al-Obaidi, K. M., Ismail, M. and Abdul Rahman, A. M. (2014). Passive cooling techniques through reflective and radiative roofs in tropical houses in Southeast Asia: A literature review, Frontiers of Architectural Research, 3(3), pp. 283–297. http://dx.doi.org/10.1016/j.foar.2014.06.002

[25] Chung, M., Park, J. and Ko, M. (2015). Effect of the solar radiative properties of existing building roof materials on the energy use in humid continental climates. Energy and Buildings, 102, pp. 172-180. https://doi.org/10.1016/j.enbuild.2015.05.022

[26] Alchapar, N. L. and Correa, E. N. (2016). Aging of roof coatings . Solar reflectance stability according to their morphological characteristics, Construction and Building Materials, 102, pp. 297–305. http://dx.doi.org/10.1016/j.conbuildmat.2015.11.005

[27] WeatherCompanyLLC (2014) ESTACIÓN METEOROLÓGICA IELOROEL2(ElCambio). Available at: https://www.wunderground.com/personal-weather-station/dashboard?ID=IELOROEL2#history (Accessed: December 24, 2016).

[28] Wilson, A. M. and Jetz, W. (2016). Remotely Sensed High-Resolution Global Cloud Dynamics for Predicting Ecosystem and Biodiversity Distributions, PLOS Biology, 14(3): e1002415. https://doi.org/10.1371/journal.pbio.1002415

[29] Wacker, S., Gröbner, J., Zysset, C., Diener, L., Tzoumanikas, P., Kazantzidis, A., Vuilleumier, L., Stöckli, R., Nyeki, S. and Kämpfer, N. (2015). Cloud observations in Switzerland using hemispherical sky cameras, Journal of Geophysical Research, 120, pp. 695–707. http://doi:10.1002/2014JD022643

[30] Luiz, E. W., Martins, F. R., Costa, R. S. and Pereira, E. B. (2018). Comparison of methodologies for cloud cover estimation in Brazil - A case study, Energy for Sustainable Development, 43, pp. 15–22. https://doi.org/10.1016/j.esd.2017.12.001

[31] Beckers, B. and Masset, L. (2003). HeliodonTM_2.6-1 software. Available at: www.heliodon.net (Accessed: January 12, 2016)

[32] InstitutoEcuatorianodeNormalización(INEN) (2008). NTE_INEN 2221:Paneles de Acero. Requisitos. Quito, Ecuador: INEN.

[33] American Society for Testing and Materials(ASTM) (2007). Criterios ASTM para Productos Planchas de Acero Recubiertos. West Conshohocken, PA: ASTM International. Available at: www.astm.org

[34] ASHRAE (2001). Handbook of Fundamentals. Thermal radiation-Heat transfer (Chapter 3).

[35] Bergman, T., Lavine, A., Incropera, F. and Dewitt, D. (2011). Fundamentals of Heat and Mass Transfer. Danvers: John Wiley & sons.

[36] NOVACERO (2016). CATÁLOGO DE PRODUCTOS NOVACERO. Available at: www.novacero.com (Accessed: 1 June 2016).

[37] Simpson, J. R. and McPherson, E. G. (1997). The effects of roof albedo modification on cooling loads of scale model residences in Tucson, Arizona, Energy and Buildings, 25(2), pp. 127–137. https://doi.org/10.1016/S0378-7788(96)01002-X

[38] López, J., Isalgué, A., Coch, H., and Alonso, C. (2014). Yellow is green: An opportunity for energy savings through colour in architectural spaces, Energy and Buildings, 78, pp 105-112. https://doi.org/10.1016/j.enbuild.2014.04.011

[39] Baneshi, M., Gonome, H. and Maruyama, S. (2016). Cool black roof impacts into the cooling and heating load demand of a residential building in various climates, Solar Energy Materials and Solar Cells, 152, pp. 21–33. http://dx.doi.org/10.1016/j.solmat.2016.03.023

[40] Vollmer, M., Möllmann, K. (2010). Infrared Thermal Imaging: Fundamentals, Reserach and Aplications. Weinheim-Germany: WILEY-VCH.

[41] ASTM Designation: E1933-99a (1999), Standard Test Methods for Measuring and Compensating for Emissivity Using Infrared Imaging Radiometers[1].

[42] Dimoudi, A., Androutsopoulos, A. and Lykoudis, S. (2006) .Summer performance of a ventilated roof component, Energy and Buildings, 38, pp. 610–617. https://doi.org/10.1016/j.enbuild.2005.09.006

[43] Gagliano, A., Patania, F., Nocera, F., Ferlito, A. and Galesi, A. (2012) .Thermal performance of ventilated roofs during summer period, Energy and Buildings, 49, pp. 611–618. https://doi.org/10.1016/j.enbuild.2012.03.007

[44] Adobe (2017). Adobe Photoshop 10.0. Available at: www.adobe.com/es/ (Accessed: January 12, 2016)

[45] DesignBuilder (2016). DesignBuilder Software Ltd - Home. Available at: https://www.designbuilder.co.uk/ (Accessed: January 12, 2016)

[46] DOE (2017). EnergyPlus Licensing | EnergyPlus. Available at: https://energyplus.net/licensing (Accessed: January 12, 2016)

[47] Torres, J. (2018). Comportamiento térmico de la cubierta en un clima cálido húmedo. Repercusion energética en el edificio. Politechnic University of Catalonia, Barcelona, Spain. Available at: http://hdl.handle.net/10803/664053

[48] INSTH. (1994). NTP 345: Ventilation assessment using tracer gases.

[49] Suehrcke, H., Peterson, E. L. and Selby, N. (2008). Effect of roof solar reflectance on the building heat gain in a hot climate, Energy and Buildings, 40(12), pp. 2224–2235. https://doi.org/10.1016/j.enbuild.2008.06.015

[50] Zingre, K. T., Wan, M. P., Wong, S. K., Toh, W. B. T. and Lee, I. Y. L. (2014). Modeling of cool roof heat transfer in tropical climate, Energy, 82, pp. 813–826. http://dx.doi.org/10.1016/j.renene.2014.09.045

[51] Torres-Quezada, J., Pages, A., Coch, H. and Isalgué, A. (2016). Radiative Performance assessment of two roofs in Meditarranean and Equatorial climates. In First International Conference on Urban Physics, pp. 337–348.

[52] Torres-Quezada, J., Coch, H. and Isalgué, A. (submitted). Data set of climatic factors measured in a low latitude region with warm and humid climate: solar radiation, cloud cover and sky temperature. Energy and Buildings *Data in Brief*.